Chemical Physics Letters 754 (2020) 137677

Contents lists available at ScienceDirect

Chemical Physics Letters

journal homepage: www.elsevier.com/locate/cplett

Research paper

Structural characterization and electronic properties of Ru-doped Cu_n (n = 1–12) clusters

J.A. Morato-Márquez[a], Srinivas Godavarthi[b], Claudia G. Espinosa-González[b], José G. Torres-Torres[a], A.R. Rodríguez-Domínguez[c], A. Muñoz-Castro[d], Filiberto Ortiz-Chi[b,*], P.L. Rodríguez-Kessler[d,*]

[a] DACB-Laboratorio de Nanomateriales Catalíticos Aplicados al Desarrollo de Fuentes de Energía y Remediación Ambiental, Universidad Juárez Autónoma de Tabasco, Cunduacán 86690, Tabasco, México
[b] CONACYT-Universidad Juárez Autónoma de Tabasco, Centro de Investigación de Ciencia y Tecnología Aplicada de Tabasco, Cunduacán 86690, Tabasco, México
[c] Instituto de Física, Universidad Autónoma de San Luis Potosí, San Luis Potosí 78000, México
[d] Grupo de Química inorgánica y Materiales Moleculares, Facultad de Ingeniería, Universidad Autónoma de Chile, El Llano Subercaseaux 2801, Santiago 8900000, Chile

HIGHLIGHTS

- Two global search approaches perform the exploration of the potential energy surface.
- Structural prediction of Ru-doped Cun clusters from n = 1 to 12.
- Ru atom always occupies the highest coordinated position in the global minima.
- Putative global minimum for RuCu12 is an icosahedron with the Ru atom in the center.
- RuCu10 exhibits the highest structural and chemical stability from the series.
- Compared with their pure copper counterparts, copper clusters doped with Ru atoms significantly enhance their reactivity.

ABSTRACT

We investigate the structural, electronic, and chemical properties of Cu_n (n = 1–12) clusters doped with a single Ru atom. Geometry after global optimizations for $RuCu_n$ clusters, at n < 7, is similar to the corresponding for pure Cu_{n+1}. From n = 8 to 10, the Ru atom is highly coordinated, coming from dome-shaped structures to their total encapsulation. Energetic descriptors suggest that $RuCu_{10}$ has the highest stability from the series. HOMO-LUMO gap becomes narrower for doped clusters, compared to their pure counterparts, making them more reactive. Likewise, chemical indexes confirm the reactivity improvement of the doped clusters.

1. Introduction

Transition metal clusters in the subnanometer region have attracted significant attention because of their potential properties in catalysis, sensing, and bio-labeling. Such species are useful models for identifying and rationalizing the inherent characteristics of catalytic sites to guide the construction of new catalysts with enhanced stability and activity at low-cost [1–3]. Copper is a widely used transition metal because of its outstanding mechanical and electric properties and availability at an accessible cost for practical applications [4]. In the context of catalysis, small Cu clusters and nanoparticles have been found active for different reactions due to the high concentration of active sites and a favorable metal-support interaction [5]. In particular, Cu clusters have shown enhanced activities for CO_2 photo-reduction [6,7] and water–gas shift activity [8].

Recently, Caballero and coworkers [9] explored the energy landscape by characterizing the interaction of a CO_2 molecule with a Cu_5 cluster supported on a TiO_2 surface and found that the Cu atoms catalyze the CO_2 through C═O bond activation and a reduction of the energy barrier for bond breaking. This is because the TiO_2-supported Cu_5 cluster donates electron charge to a physisorbed CO_2 molecule when illuminated with visible light, which is further beneficial for CO_2 activation. On the other hand, the usage of single noble metal dopants in a copper surface or host has been proposed as an economical technique to improve the properties of the catalyst. Cao and coworkers [10] found that Pd-doped Cu nanoparticles reduce the activation energy of H_2 dissociation. In our previous work, we have investigated Pd-doped Cu_n (n = 3–12) clusters and found that the Pd atom always remains in

* Corresponding authors.
E-mail addresses: fortiz@conacyt.mx (F. Ortiz-Chi), rodriguezkessler.p@gmail.com (P.L. Rodríguez-Kessler).

https://doi.org/10.1016/j.cplett.2020.137677
Received 7 April 2020; Received in revised form 19 May 2020; Accepted 1 June 2020
Available online 03 June 2020
0009-2614/ © 2020 Elsevier B.V. All rights reserved.

the cluster surface, including isomerization effects at specific sizes. Analysis of the electronic structure and the spin-polarization density isosurface identified active sites in the clusters [11].

Lately, Cu_nRu_m bimetallic clusters have been found to maximize the catalytic activity for hydrogen evolution reaction (HER), offering a new approach for achieving high performance at low-cost [12]. Such alloys can exhibit outstanding HER activity in comparison to commercial Pt-catalyst in basic media, making the study of small Cu_nRu_m clusters relevant to provide a deeper understanding of the possible catalytic sites along the alloy surface. Also, Ru-doped Cu is a catalyst in various selective reactions, such as the hydrogenation of glucose, citral, and alginic acid [13–15]. Karagiannis and coworkers [16] studied the structural, electronic, and optical properties of neutral, cationic, and anionic bimetallic Ru−Cu clusters in the framework of the time-dependent DFT. The results of thermodynamic stability, electronic absorption spectra, and low-lying electronic states were in good agreement with experimental data.

The progress in nanocatalysis and catalytic systems requires research on different noble metal dopants from the fundamental point of view. Herein, we set to address the evolution of the structural and electronic properties for Ru-doped Cu_n clusters up to n = 12, as a first approximation to characterize catalytic sites retaining a low dopant ratio where the Ru-atom is exposed for further interaction towards reactants. The putative global minimum for these clusters was determined to perform a stochastic search for each size and corroborated the global minimum with the simulated annealing method. Results show that, with the increase in size, Ru impurity tends to be incorporated at a central site within the cluster towards a complete encapsulation. The geometry and electronic properties of the clusters are discussed in detail.

2. Computational details

Global minimum search for each cluster size was performed in two approaches, a stochastic kick strategy and later corroborated with the simulated annealing method. The stochastic approach was carried out using the GLobal Optimization of MOlecular Systems (GLOMOS). GLOMOS is written in python and includes a set of methodologies to find the global minimum in atomic and molecular systems, where the DFT local optimizations are solved using electronic structure codes such as Gaussian [17] or VASP [18,19]. The number of initial structures was set equal to 50 times the number of atoms in the cluster, i.e., for $RuCu_{12}$, the number of initial trial structures was 650. Simulated annealing (SA), based on ab-initio molecular dynamics (AIMD), is used to corroborate the results. More details of the SA method can be found in our previous work [11]. In a second optimization stage, all the cluster geometries obtained in both global search schemes were discriminated by similarity and fully optimized with the B3PW91 [20] hybrid functional and the triple zeta def2-TZVP [21] basis set; including the DFT-D3 empirical dispersion correction proposed by Grimme [22]. Harmonic vibrational frequencies were computed to verify that the optimized structures have no imaginary frequencies. Five different spin multiplicities were considered for each structure to identify the lowest in energy configuration.

3. Results

3.1. Structural properties

The first row in Fig. 1 shows the lowest energy structures for the $RuCu_n$ (n = 3–12) clusters, while the second row illustrates, the next low energy isomer. The putative global minimum (GM) structure on each cluster includes information about the spin multiplicity, point group, and average binding energy. Subsequent low-lying energy isomer includes the spin multiplicity, point group, and relative energy difference (ΔE) respect to the GM geometry. As a general trend, for all the lowest energy clusters, the Ru atom always occupies the highest coordination position. Interestingly, for $RuCu_n$ (n = 3–6) clusters, the coordination for the Ru atom is the highest possible, equal to the number of copper atoms.

Therefore, in the series of doped clusters, the coordination number of the Ru atom increases linearly with n, from 1 to 6, maintaining this atomic coordination even in the largest clusters. The GM structures of the present systems are consistent with those reported by other pure metal clusters. For example, $RuCu_2$ takes the form of a distorted triangle, $RuCu_3$ is a planar rhombus, $RuCu_4$ a planar trapezoid, $RuCu_5$ a side-capped trigonal bipyramid, $RuCu_6$ a pentagonal bipyramid, $RuCu_7$ a capped pentagonal bipyramid, and $RuCu_8$ a three capped octahedron (or bicapped pentagonal bipyramid). We found that $RuCu_{9\text{-}12}$ clusters favor the formation of Ru encapsulated structures leading to a complete icosahedron on $RuCu_{12}$.

For comparison, we have performed full-optimization calculations on Cu_{n+1} (n = 3–12) clusters, whose global minimum structures are available in the literature [23]. In the process, we found that the B3PW91/def2-TZVP approach favors different GM structures for Cu_8 and Cu_9 clusters, as shown in Fig. 2. We attribute the difference because, in Ref. [23], the Authors have employed a periodic DFT approach and a different functional; however, a more detailed analysis by using several functionals would be useful to provide a more definitive assignment of the GM structure. By analyzing the putative GM for the bimetallic $RuCu_n$ structures on n = 2–6 and 8, we find a similar shape compared to the pure Cu_{n+1} clusters, as reported by R. Singh and coworkers [24]. These doped clusters could be constructed by replacing the more coordinate Cu atom with Ru, consequently changing the total spin magnetic moment of the system.

On the other hand, the $RuCu_n$ clusters show similar features when the Cu_n clusters are doped with another noble metal such as Pd, but only for n = 5 and 6, as shown in our previous work [11]. However, the most significant difference between the $RuCu_n$ and the $PdCu_n$ systems is observed for n = 10–12. For $RuCu_n$ (n = 10–12) clusters, the dopant metal atom is encapsulated by the copper atoms, while for $PdCu_n$ (n = 10–12) clusters, the Pd atom occupies the surface site.

Table 1 contains the minimum, maximum, and average bond lengths between Cu−Cu and Ru−Cu atoms in $RuCu_n$ clusters. For $RuCu_n$ (n = 3–7, and 9) clusters, the average bond length between Ru and Cu atoms is longer than the corresponding one between copper atoms. The situation is the opposite for n = 2, 8, and 10–12. In particular, when the Ru atom presents the total encapsulation (n = 10–12), the bond distances show differences by more than 0.1 Å. This result suggests a degree of hybridization between the Ru atom and the Cu_n host. It is worth noting that for pure Cu_{n+1} (n = 3–12) clusters, the average bond length between Cu−Cu atoms is shorter than in $RuCu_n$ (n = 3–12) clusters, which is consistent with the cage structure formation.

Regarding the magnetic evolution of the Cu_{n+1} system, previously reported, an oscillatory behavior between 0 and 1 μB has been attributed to the electron parity effect [23]. Similarly, most of the copper clusters doped with a Ru atom (n = 1–9, and 13) exhibit an oscillatory behavior in their total spin magnetic moment, from 2 to 3 μB, corresponding to triplet and quadruplet multiplicities. Two exceptions occur in $RuCu_{10}$ and $RuCu_{11}$ clusters, with 0 and 1 μB values, respectively, corresponding to singlet and doublet multiplicities.

3.2. Energetics

To determine the computational accuracy on the $RuCu_n$ system, we have performed a comparison on the bond length and binding energy of the Cu_2 dimer. Our computations show that Cu_2 dimer has a bond length of 2.47 Å and binding energy of 0.86 eV/atom, in good agreement with previous theoretical and experimental studies [25–29]. Results show that RuCu dimer has 3 μB of the magnetic moment, larger than for the Cu_2 dimer (1 μB). The observed values of the Ru−Cu bond length (2.22 Å), and the binding energy (0.81 eV/atom), suggest that

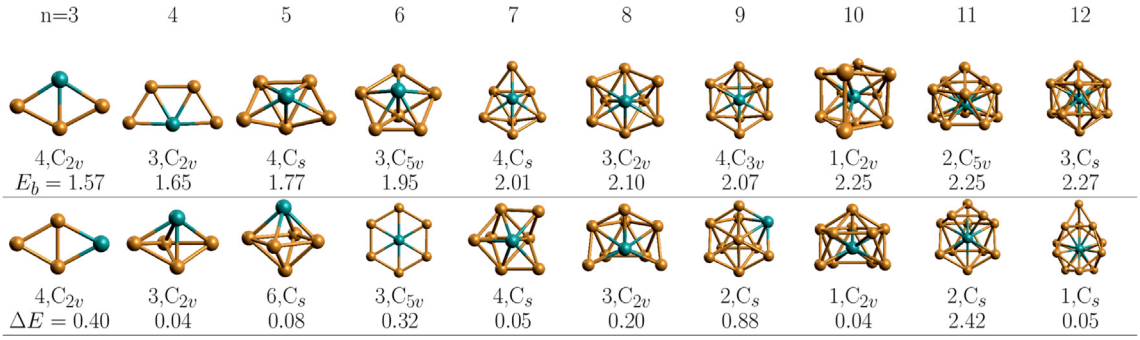

Fig. 1. In the first row, the GM for the $RuCu_n$ clusters as a function of size, including the spin multiplicity, point group, and average binding energy (eV/atom). In the second row, the next low-lying energy isomer, including the magnetic moment, point group, and energy difference (eV) respect to the GM structure.

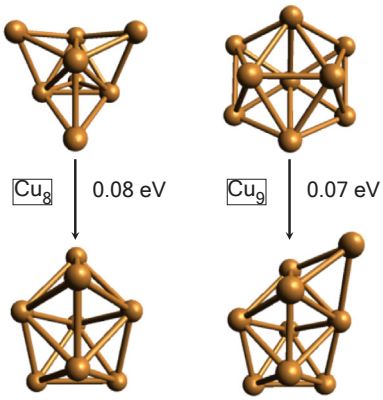

Fig. 2. Changes in the global minima for the Cu_8 and Cu_9 clusters, with respect to the previously reported ones [23]. All structures were fully-optimized at the B3PW91/def2-TZVP level.

Table 1
Minimum (R_{min}), maximum (R_{max}), and average (R_{avg}) bond lengths between the Cu−Cu and Ru−Cu bonds in the $RuCu_n$ (n = 2–12) GM structures. All the distances are in Å.

	Cu−Ru			Cu−Cu		
n	R_{min}	R_{max}	R_{avg}	R_{min}	R_{max}	R_{avg}
2	2.41	2.41	2.41	2.49	2.49	2.49
3	2.46	2.55	2.52	2.44	2.44	2.44
4	2.50	2.54	2.52	2.44	2.48	2.46
5	2.50	2.68	2.59	2.41	2.50	2.48
6	2.53	2.55	2.53	2.50	2.55	2.52
7	2.51	2.69	2.56	2.46	2.57	2.50
8	2.48	2.60	2.52	2.46	2.56	2.53
9	2.50	2.65	2.57	2.44	2.77	2.54
10	2.41	2.44	2.42	2.60	2.77	2.65
11	2.42	2.47	2.45	2.50	2.63	2.56
12	2.48	2.49	2.48	2.54	2.69	2.61

the formation of Ru−Cu bonds in the $RuCu_n$ clusters is energetically favorable.

Thermodynamic stability of the $RuCu_n$ clusters is further investigated by calculating the binding energy per atom (E_b), second-order energy differences (Δ_2E), and fragmentation energy (E_f), which are defined as:

$$E_b = (nE[Cu] + E[Ru] - nE[RuCu_n])/(n+1), \quad (1)$$

$$\Delta_2E = E[RuCu_{n+1}] + E[RuCu_{n-1}] - 2E[RuCu_n], \quad (2)$$

$$E_f = E[RuCu_{n-1}] + E[Cu_n] - E[RuCu_n], \quad (3)$$

where E[Cu], E[Ru], and E[$RuCu_n$] are total energies of an isolated Cu atom, the Ru atom, and the $RuCu_n$ cluster, respectively. Fig. 3 compares

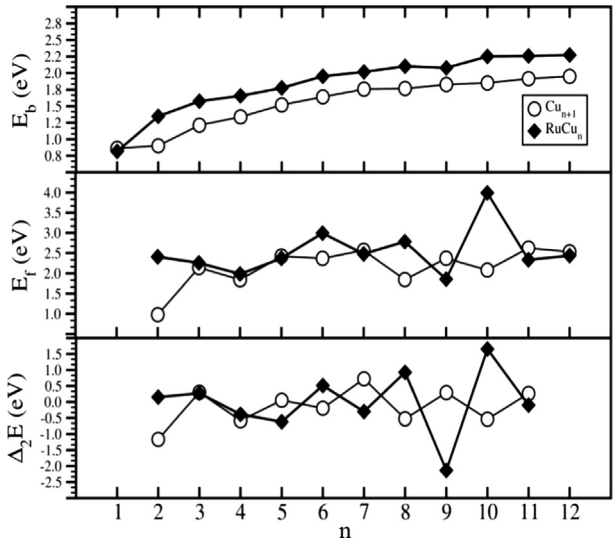

Fig. 3. Average binding energy (E_b), dissociation energy (E_f), and second-order energy differences (Δ_2E) for the $RuCu_n$ and Cu_{n+1} clusters as a function of size (n).

the binding energy, fragmentation energy, and second-order energy differences between the $RuCu_n$ and the Cu_{n+1} clusters, with n = 1–12. The binding energy for the $RuCu_n$ and Cu_{n+1} clusters shows a similar behavior, a monotonous increment as a function of the size, with variations between 0.3 and 0.4 eV. The evolution of the binding energy curve suggests that the subsequent addition of more copper atoms is energetically favorable. Fragmentation processes may involve dissociation barriers. When the fragmentation energy is negative, the parent clusters are unstable and could dissociate spontaneously by a quantity equal to $|E_f|$. In this work, all the clusters have positive fragmentation energies, implying that they are stable and resistant toward fragmentation. Fragmentation energy differences between doped and pure clusters are significant (1.43 and 1.91 eV, respectively) at n = 2 and n = 10, slight (0.93–0.51 eV) at n = 6, 8, and 9, and despicable (not higher than 0.2 eV) for the rest. It is important to note that the most significant difference corresponds to n = 10, the first fully encapsulated structure for the doped clusters. So, it is inferred that both systems of clusters are difficult to dissociate; however, the $RuCu_{10}$ case is especially hard.

Frequently, the second-order energy difference (Δ_2E) is used to quantify the relative stability of the clusters. For n > 3, the Δ_2E of the even-numbered Ru-doped clusters are more stable than the odd-numbered. The $RuCu_9$ structure has a negative second-order energy difference, which means that this is less stable than its neighboring clusters. In counterpart, $RuCu_{10}$ cluster has a high significant value, demonstrating once again its high stability.

Table 2
Values of the vertical ionization potential (vIP), vertical electron affinity (vEA), highest occupied molecular orbital (ε_H), lowest unoccupied molecular orbital (ε_L), and the Δ_{H-L} gap for the $RuCu_n$ and Cu_{n+1} clusters. All parameters are in eV.

	$RuCu_n$					Cu_{n+1}					
n	vIP	vEA	$-\varepsilon_H$	$-\varepsilon_L$	Δ_{H-L}	vIP	IP (exp)	vEA	$-\varepsilon_H$	$-\varepsilon_L$	Δ_{H-L}
1	6.77	1.43	5.41	2.53	2.88	7.89	7.89 ± 0.01[a]	0.70	5.67	2.31	3.35
2	7.95	0.74	5.42	2.42	3.00	5.90	5.8 ± 0.1[b]	0.75	4.09	2.76	1.33
3	6.31	0.99	4.61	2.79	1.83	6.59	7.15 ± 0.7[c]	1.29	4.83	2.79	2.04
4	6.65	1.31	5.17	2.93	2.24	6.29	6.3 ± 0.1[b]	1.64	4.67	2.19	2.48
5	6.40	1.77	4.51	3.05	1.46	7.11	7.15 ± 0.7[c]	1.04	5.54	2.27	3.26
6	6.33	1.36	4.98	3.10	1.88	6.03	6.1 ± 0.1[b]	1.59	4.48	2.13	2.35
7	5.91	1.85	4.63	2.42	2.21	6.91	6.4–7.9[b]	0.90	5.41	2.07	3.34
8	5.80	1.72	4.62	2.34	2.28	5.42	5.3 ± 0.1[b]	1.41	4.00	2.75	1.25
9	4.83	2.21	3.69	2.61	1.08	5.92	6.1 ± 0.1[b]	1.24	4.52	2.56	1.96
10	5.91	0.95	4.93	1.89	3.04	5.88	–	2.05	4.54	2.71	1.83
11	4.41	1.17	3.41	2.31	1.10	6.09	–	1.80	4.76	3.02	1.74
12	4.57	1.50	3.60	2.52	1.08	5.63	–	2.03	4.36	2.78	1.58

[a] From Ref. [30].
[b] From Ref. [31].
[c] From Ref. [32].

3.3. Electronic properties

The HOMO-LUMO gap is an important parameter to examine the chemical stability of the clusters. Table 2 shows the energy values for the highest occupied molecular orbital ($-\varepsilon_H$) and the lowest unoccupied molecular orbital ($-\varepsilon_L$), as well as the gap between them (Δ_{H-L}). Compared with their Cu_6 and Cu_8 pure counterparts, for $RuCu_5$ and RuCu7 clusters, Δ_{H-L} decreased dramatically by 1.8 and 1.3 eV, respectively; this is particularly striking because the corresponding GM structures have the same geometry. In most cases, Δ_{H-L} decreases for the doped systems, which means that the structures could become much more chemically reactive. Nevertheless, for n = 2, 8, and 10 the gap increased more than 1 eV, making these structures less reactive. In a particular case, $RuCu_{10}$ exhibits a high Δ_{H-L} value associated with the singlet state, being more stable than the other spin configurations. We find that the $RuCu_{10}$ GM structure shows a decrease in its gap for higher multiplicities.

Vertical ionization potential (vIP) and vertical electron affinity (vEA) are two important factors to get insight into the electronic properties. These properties given information about the energy of the system by removing or adding an electron but maintaining the geometry. The vIP and vEA can be calculated as follows:

$$vIP = E_{cation} - E_{neutral}, \quad (4)$$

$$vEA = E_{neutral} - E_{anion}. \quad (5)$$

Fig. 4 displays the vIP and vEA evolution, and Table 2 resume their values. The values regarding the vIP are found in excellent agreement with the available experimental data which helped us to validate the accuracy of the computations [30–33]. The vIP show an even/odd oscillation behavior for the smaller clusters, a response that decreases as the number of atoms increases. The $RuCu_n$ and Cu_{n+1} clusters with even n-values have a similar vIP, in the range from n = 3 to 10, with differences less than 1.1 eV. Especially, $RuCu_{10}$ presents the same vIP as its Cu_{11} counterpart (28 meV difference). In contrast, respect to their pure counterparts, the vIP for the doped cluster at n = 2 is about 2 eV above, while at n = 11 it is 1.68 eV below. Compared with their pure counterparts, the energy required to remove an electron in doped clusters with n > 7 is generally less, once again showing the high kinetic stability of dome-shaped structures with encapsulation of the noble metal. On the other hand, the vEA behavior for the doped clusters presents a rapid growth from n = 2 to 5. It then begins to have an oscillatory behavior, which increases remarkably at n = 10. Average vEA values for doped clusters, from n = 1 to 6, do not exceed in more than 0.73 eV to their pure counterparts. For the pure clusters, from

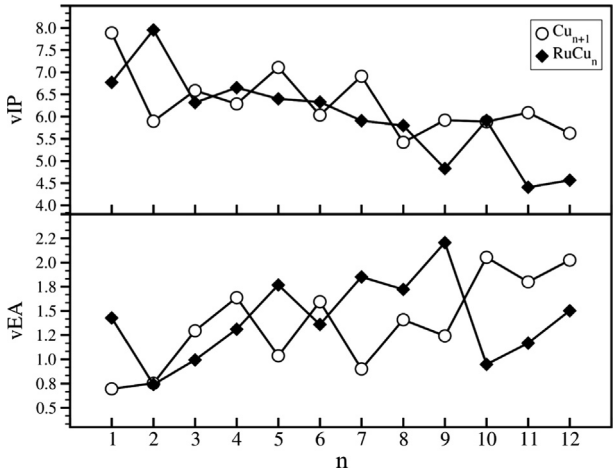

Fig. 4. Vertical ionization potential (vIP) and vertical electron affinity (vEA) for the $RuCu_n$ and Cu_{n+1} clusters as a function of the size (n).

n = 7 to 9, the vEA values are lower than the doping ones. The opposite happens from n = 10 to 12, where $RuCu_{10}$ has the most notable difference (1.1 eV) respect to its pure counterpart. The vEA varies in a range between 0.73 and 0.30 eV, so that both systems of clusters, Cu_{n+1} and $RuCu_n$, have similar energy barriers to accept an electron from the surroundings.

3.4. Chemical descriptors

Chemical potential, chemical hardness, and electrophilicity are some indices that help us to understand the chemical reactivity in clusters. Chemical potential μ measures the tendency of the electrons to escape from an equilibrium system [34]. Secondly, chemical hardness η is a global property that measures the resistance of the system to changes in its electronic distribution [35]. Finally, the electrophilicity index ω quantifies the energetic stability of a system saturated with electrons from the external environment [36]. As a numerical approach, μ, η, and ω were calculated based upon the finite difference approximation of Parr et al. [37] as follows:

$$\mu = -\frac{vIP + vEA}{2}, \quad (6)$$

$$\eta = (vIP - vEA), \quad (7)$$

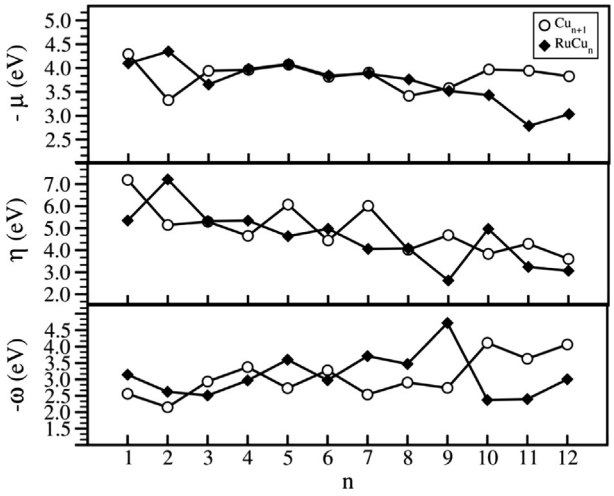

Fig. 5. Chemical potential (μ), chemical hardness (η), and the electrophilicity index (ω) for the Cu_{n+1} and $RuCu_n$ clusters as a function of the size (n).

$$\omega = -\frac{\mu^2}{2\eta}. \quad (8)$$

Chemical hardness (Eq. (7)) was written without the 1/2 factor, following more current references [38–40]. Figure 5 shows the chemical potential, chemical hardness, and electrophilicity for the doped clusters. The chemical potential has an extremely smooth oscillatory behavior, reaching maximum and minimum values for the even and odd n values, respectively. Nevertheless, on average, μ tend to stay around 3.83 eV. The μ values for the pure clusters also present smaller oscillations, but tending to decrease, first slightly from n = 4 to 9, and more dramatically from n = 10 to 12 (~1.5 eV). Molecular hardness for doped clusters is, in comparison, mostly higher than that for their pure counterparts. Doped clusters have a slight variation in η (from 2 to 3.5 eV). For both systems of clusters, η decreases oscillatory with the addition of copper atoms. The electrophilicity index has a similar behavior to the vEA, which confirms that the cluster stability is correlated with the acceptance of electrons. Chemical descriptors suggest that the clusters where the Ru atom is encapsulated, in a dome, and core–shell structures present high chemical reactivity.

4. Conclusions

In this work, we have studied the structural and electronic properties of Ru-doped Cu_n clusters from n = 1 to 12. Extensive searches identified the lowest energy structures, for each corresponding energy landscape, at the B3PW91/def2-TZVP level. In the doped clusters, the Ru atom always occupies the highest coordinated position until reaching the limit value of six in $RuCu_6$ and keeping this value for n > 6. The tendency of the Ru atom to occupy the most coordinated sites leads to the formation of endohedral structures from $RuCu_8$, to an icosahedron in $RuCu_{12}$. The binding energy shows a monotonous increment as a function of the cluster size, suggesting that the progressive growth of larger clusters (up to n = 12) is energetically favorable. Compared with their bare counterparts, doped clusters have higher binding energies. Energetic descriptors suggest that the $RuCu_{10}$, the first where the Ru atom is encapsulated, has the highest stability from the series of doped clusters.

Electronic and reactivity parameters show an oscillatory behavior, depending on the even or odd number of Cu atoms in the $RuCu_n$ clusters. The energy to remove one electron from the doped clusters, up to n = 9, is smaller than that for pure Cu clusters. The behavior of the electrophilicity index indicates that all the $RuCu_n$ clusters, from n = 1 to 12, have similar barriers to accept surrounding electrons. Chemical descriptors suggest that the geometries where the Ru atom is encapsulated show high chemical reactivity. Based on these results, we can infer that Cu systems doped with Ru atoms significantly increase their reactivity, which can be useful in various applications in the area of catalysis.

CRediT authorship contribution statement

J.A. Morato-Márquez: Investigation, Validation, Visualization, Writing - original draft. **Srinivas Godavarthi:** Supervision, Writing - review & editing. **Claudia G. Espinoza-González:** Investigation. **J. Gilberto Torres-Torres:** Funding acquisition, Resources, Supervision. **A.R. Rodríguez-Domínguez:** Conceptualization. **A. Muñoz-Castro:** Supervision. **Filiberto Ortiz-Chi:** Funding acquisition, Project administration, Conceptualization, Supervision, Methodology, Software, Writing - review & editing. **P.L. Rodríguez-Kessler:** Conceptualization, Supervision, Validation, Methodology, Software, Writing - review & editing.

Declaration of Competing Interest

The authors declare that they have no known competing financial interests or personal relationships that could have appeared to influence the work reported in this paper.

Acknowledgements

The authors thank CONACyT (grant Al-S-26876) for financial support. The JUCHIMAN (CONACyT, grant U0003-2015-7-26609) and KUKULCAN (CONACyT, grant CB-2015-252356) are gratefully acknowledged for the allocation of computational resources. J.A.M.-M. thanks to CONACyT for his Master scholarship. F.O.-C. thanks the SEP-PFCE-UJAT-2018 project and the Cátedras-CONACyT 1024 project. A.M.-C acknowledges to FONDECYT 1180683 grant. P.L.R.-K acknowledges to FONDECYT 3190329 grant.

Appendix A. Supplementary material

Supplementary data to this article can be found online at https://doi.org/10.1016/j.cplett.2020.137677.

References

[1] E. Jimenez-Izal, B.C. Gates, A.N. Alexandrova, Designing clusters for heterogeneous catalysis, Phys. Today 72 (2019) 38–43, https://doi.org/10.1063/PT.3.4248.
[2] O. Hübner, H.-J. Himmel, Metal cluster models for heterogeneous catalysis: a matrix-isolation perspective, Chem. – A Eur. J. 24 (2018) 8941–8961, https://doi.org/10.1002/chem.201706097.
[3] E. Jimenez-Izal, A.N. Alexandrova, Computational design of clusters for catalysis, Annu. Rev. Phys. Chem. 69 (2018) 377–400, https://doi.org/10.1146/annurev-physchem-050317-014216.
[4] A.A.B. Padama, J.D. Ocon, H. Nakanishi, H. Kasai, Interaction of CO, O, and CO_2 with Cu cluster supported on Cu(1 1 1): A density functional theory study, J. Phys. Condens. Matter. 31 (2019) 415201, https://doi.org/10.1088/1361-648X/ab2b66.
[5] S.K. Iyemperumal, N.A. Deskins, Activation of CO_2 by supported Cu clusters, Phys. Chem. Chem. Phys. 19 (2017) 28788–28807, https://doi.org/10.1039/C7CP05718K.
[6] D. Liu, Y. Fernández, O. Ola, S. Mackintosh, M. Maroto-Valer, C.M.A. Parlett, A.F. Lee, J.C.S. Wu, On the impact of Cu dispersion on CO_2 photoreduction over Cu/TiO_2, Catal. Commun. 25 (2012) 78–82, https://doi.org/10.1016/j.catcom.2012.03.025.
[7] C. Liu, S.K. Iyemperumal, N.A. Deskins, G. Li, Photocatalytic CO_2 reduction by highly dispersed Cu sites on TiO_2, J. Photon. Energy 7 (2016) 012004, https://doi.org/10.1117/1.JPE.7.012004.
[8] J.B. Park, J. Graciani, J. Evans, D. Stacchiola, S.D. Senanayake, L. Barrio, P. Liu, J.F. Sanz, J. Hrbek, J.A. Rodriguez, Gold, copper, and platinum nanoparticles dispersed on CeO_x/TiO_2(110) surfaces: high water-gas shift activity and the nature of the mixed-metal oxide at the nanometer level, J. Am. Chem. Soc. 132 (2010) 356–363, https://doi.org/10.1021/ja9087677.
[9] P. López-Caballero, A.W. Hauser, M. Pilar de Lara-Castells, Exploring the catalytic properties of unsupported and TiO_2-supported Cu_5 clusters: CO_2 decomposition to CO and CO_2 photoactivation, J. Phys. Chem. C 123 (2019) 23064–23074, https://doi.org/10.1021/acs.jpcc.9b06620.

[10] Y. Cao, M. Zhu, P. Li, R. Zhang, X. Li, Q. Gong, K. Wang, M. Zhong, D. Wu, F. Lin, H. Zhu, X. Cao, Q. Fu, Y. Luo, Catalytic activity of Pd-doped Cu nanoparticles for hydrogenation as a single-atom-alloy catalyst, Phys. Chem. Chem. Phys. 16 (2014) 8367–8375, https://doi.org/10.1039/c4cp00399c.
[11] P.L. Rodríguez-Kessler, P. Alonso-Dávila, P. Navarro-Santos, J.A. Morato-Márquez, F. Ortíz-Chi, A.R. Rodríguez-Domínguez, Hydrogen chemisorption on Pd-doped copper clusters, J. Phys. Chem. C. 123 (2019) 15834–15840, https://doi.org/10.1021/acs.jpcc.9b03637.
[12] Q. Wu, M. Luo, J. Han, W. Peng, Y. Zhao, D. Chen, M. Peng, J. Liu, F.M.F. de Groot, Y. Tan, Identifying electrocatalytic sites of the nanoporous copper-ruthenium alloy for hydrogen evolution reaction in alkaline electrolyte, ACS Energy Lett. 5 (2020) 192–199, https://doi.org/10.1021/acsenergylett.9b02374.
[13] E. Asedegbega-Nieto, B. Bachiller-Baeza, A. Guerrero-Ruíz, I. Rodríguez-Ramos, Modification of catalytic properties over carbon supported Ru–Cu and Ni–Cu bimetallics, Appl. Catal. A Gen. 300 (2006) 120–129, https://doi.org/10.1016/j.apcata.2005.10.061.
[14] J. Liu, L.L. Zhang, J. Zhang, T. Liu, X.S. Zhao, Bimetallic ruthenium–copper nanoparticles embedded in mesoporous carbon as an effective hydrogenation catalyst, Nanoscale 5 (2013) 11044, https://doi.org/10.1039/c3nr03813k.
[15] C. Ban, S. Yang, H. Kim, D.H. Kim, Effect of Cu addition to carbon-supported Ru catalysts on hydrogenation of alginic acid into sugar alcohols, Appl. Catal. A Gen. 578 (2019) 98–104, https://doi.org/10.1016/j.apcata.2019.04.003.
[16] E.E. Karagiannis, C.E. Kefalidis, I. Petrakopoulou, C.A. Tsipis, Density functional study of structural, electronic, and optical properties of small bimetallic ruthenium-copper clusters, J. Comput. Chem. 32 (2011) 1241–1261, https://doi.org/10.1002/jcc.21705.
[17] M.J. Frisch, G.W. Trucks, H.B. Schlegel, G.E. Scuseria, M.A. Robb, J.R. Cheeseman, G. Scalmani, V. Barone, G.A. Petersson, H. Nakatsuji, X. Li, M. Caricato, A. V Marenich, J. Bloino, B.G. Janesko, R. Gomperts, B. Mennucci, H.P. Hratchian, J. V Ortiz, A.F. Izmaylov, J.L. Sonnenberg, D. Williams-Young, F. Ding, F. Lipparini, F. Egidi, J. Goings, B. Peng, A. Petrone, T. Henderson, D. Ranasinghe, V.G. Zakrzewski, J. Gao, N. Rega, G. Zheng, W. Liang, M. Hada, M. Ehara, K. Toyota, R. Fukuda, J. Hasegawa, M. Ishida, T. Nakajima, Y. Honda, O. Kitao, H. Nakai, T. Vreven, K. Throssell, J.A. Montgomery Jr., J.E. Peralta, F. Ogliaro, M.J. Bearpark, J. J. Heyd, E.N. Brothers, K.N. Kudin, V.N. Staroverov, T.A. Keith, R. Kobayashi, J. Normand, K. Raghavachari, A.P. Rendell, J.C. Burant, S.S. Iyengar, J. Tomasi, M. Cossi, J.M. Millam, M. Klene, C. Adamo, R. Cammi, J.W. Ochterski, R.L. Martin, K. Morokuma, O. Farkas, J.B. Foresman, D.J. Fox, Gaussian 16 Revision A.03, 2016.
[18] G. Kresse, J. Hafner, Ab initio molecular dynamics for liquid metals, Phys. Rev. B 47 (1993) 558–561, https://doi.org/10.1103/PhysRevB.47.558.
[19] G. Kresse, J. Furthmüller, Efficient iterative schemes for ab initio total-energy calculations using a plane-wave basis set, Phys. Rev. B 54 (1996) 11169–11186, https://doi.org/10.1103/PhysRevB.54.11169.
[20] J.P. Perdew, Y. Wang, Accurate and simple analytic representation of the electron-gas correlation energy, Phys. Rev. B 45 (1992) 13244–13249, https://doi.org/10.1103/PhysRevB.45.13244.
[21] F. Weigend, R. Ahlrichs, Balanced basis sets of split valence, triple zeta valence and quadruple zeta valence quality for H to Rn: Design and assessment of accuracy, Phys. Chem. Chem. Phys. 7 (2005) 3297, https://doi.org/10.1039/b508541a.
[22] S. Grimme, S. Ehrlich, L. Goerigk, Effect of the damping function in dispersion corrected density functional theory, J. Comput. Chem. 32 (2011) 1456–1465, https://doi.org/10.1002/jcc.21759.
[23] A.S. Chaves, G.G. Rondina, M.J. Piotrowski, P. Tereshchuk, J.L.F.F. Da Silva, The role of charge states in the atomic structure of Cu_n and Pt_n (n = 2–14 atoms) clusters: a DFT investigation, J. Phys. Chem. A 118 (2014) 10813–10821, https://doi.org/10.1021/jp508220h.
[24] R.K. Singh, T. Iwasa, T. Taketsugu, Insights into geometries, stabilities, electronic structures, reactivity descriptors, and magnetic properties of bimetallic Ni_m Cu_{n-m} (m = 1, 2; n = 3–13) clusters: comparison with pure copper clusters, J. Comput. Chem. 39 (2018) 1878–1889, https://doi.org/10.1002/jcc.25361.
[25] A.W. Pelzer, J. Jellinek, K.A. Jackson, H_2 reactions on palladium clusters, J. Phys. Chem. A 117 (2013) 10407–10415, https://doi.org/10.1021/jp403089x.
[26] G. Zanti, D. Peeters, DFT study of small palladium clusters Pd_n and their interaction with a CO ligand (n = 1–9), Eur. J. Inorg. Chem. 2009 (2009) 3904–3911, https://doi.org/10.1002/ejic.200900513.
[27] Y. Mu, Y. Han, J. Wang, J. Wan, G. Wang, Structures and magnetic properties of Pd_n clusters (n = 3–19) doped by Mn atoms, Phys. Rev. A 84 (2011) 053201, https://doi.org/10.1103/PhysRevA.84.053201.
[28] K. Balasubramanian, Spectroscopic properties of 41 electronic states of Pd_2, J. Chem. Phys. 89 (1988) 6310–6315, https://doi.org/10.1063/1.455397.
[29] K.P. Huber, G. Herzberg, Constants of diatomic molecules, Mol. Spectra Mol. Struct. Springer US, Boston, MA, 1979, pp. 8–689, , https://doi.org/10.1007/978-1-4757-0961-2_2.
[30] M.D. Morse, J.B. Hopkins, P.R.R. Langridge Smith, R.E. Smalley, Spectroscopic studies of the jet cooled copper trimer, J. Chem. Phys. 79 (1983) 5316–5328, https://doi.org/10.1063/1.445694.
[31] M.B. Knickelbein, Electronic shell structure in the ionization potentials of copper clusters, Chem. Phys. Lett. 192 (1992) 129–134, https://doi.org/10.1016/0009-2614(92)85440-L.
[32] D.E. Powers, S.G. Hansen, M.E. Geusic, D.L. Michalopoulos, R.E. Smalley, Supersonic copper clusters, J. Chem. Phys. 78 (1983) 2866–2881, https://doi.org/10.1063/1.445273.
[33] K. Jug, B. Zimmermann, P. Calaminici, A.M. Köster, Structure and stability of small copper clusters, J. Chem. Phys. 116 (2002) 4497–4507, https://doi.org/10.1063/1.1436465.
[34] R.F. Nalewajski, J. Korchowiec, A. Michalak, Reactivity criteria in charge sensitivity analysis, 1996, pp. 25–141. 10.1007/3-540-61131-2_2.
[35] W. Yang, R.G. Parr, Hardness, softness, and the fukui function in the electronic theory of metals and catalysis, Proc. Natl. Acad. Sci. 82 (1985) 6723–6726, https://doi.org/10.1073/pnas.82.20.6723.
[36] R.G. Parr, L.V. Szentpály, S. Liu, Electrophilicity index, J. Am. Chem. Soc. 121 (1999) 1922–1924, https://doi.org/10.1021/ja983494x.
[37] J.-L. Calais, Density-functional theory of atoms and molecules, in: R.G. Parr, W. Yang, Oxford University Press, New York, Oxford, 1989. Int. J. Quantum Chem. 47 (1993) 101–101. 10.1002/qua.560470107.
[38] P.K. Chattaraj, U. Sarkar, D.R. Roy, Electrophilicity index, Chem. Rev. 106 (2006) 2065–2091, https://doi.org/10.1021/cr040109f.
[39] S. Pan, M. Solà, P.K. Chattaraj, On the validity of the maximum hardness principle and the minimum electrophilicity principle during chemical reactions, J. Phys. Chem. A 117 (2013) 1843–1852, https://doi.org/10.1021/jp312750n.
[40] R. Saha, S. Pan, P. Chattaraj, Statistical significance of the maximum hardness principle applied to some selected chemical reactions, Molecules 21 (2016) 1477, https://doi.org/10.3390/molecules21111477.